THE JOURNAL OF CHEMICAL PHYSICS **132**, 244701 (2010)

Initiation of a passivated interface between hafnium oxide and In(Ga)As(0 0 1)−(4×2)

Jonathon B. Clemens,[1,a)] Sarah R. Bishop,[1,b)] Joon Sung Lee,[2,c)] Andrew C. Kummel,[1,d)] and Ravi Droopad[3,e)]
[1] *Department of Chemistry and Biochemistry, University of California, San Diego, 9500 Gilman Dr., 0358, La Jolla, California 92093-0358, USA*
[2] *Department of Chemistry and Biochemistry/Materials Science and Engineering Program, University of California, San Diego, 9500 Gilman Dr., 0358, La Jolla, California 92093-0358, USA*
[3] *Department of Physics, Texas State University-San Marcos, San Marcos, Texas 78666, USA*

(Received 30 November 2009; accepted 19 April 2010; published online 23 June 2010)

Hafnium oxide interfaces were studied on two related group III rich semiconductor surfaces, InAs(0 0 1)−(4×2) and $In_{0.53}Ga_{0.47}As$(0 0 1)−(4×2), via two different methods: reactive oxidation of deposited Hf metal and electron beam deposition of HfO_2. The interfaces were investigated with scanning tunneling microscopy and spectroscopy (STS). Single Hf atom chemisorption sites were identified that are resistant to oxidation by O_2, but Hf islands are reactive to O_2. After e^- beam deposition of $\leqslant 1$ ML of HfO_2, single chemisorption sites were identified. At low coverage (<1 ML), the n-type and p-type HfO_2/InGaAs(0 0 1)−(4×2) interfaces show p-type character in STS, which is typical of clean InGaAs(0 0 1)−(4×2). After annealing below 200 °C, full coverage HfO_2/InGaAs(0 0 1)−(4×2) (1–3 ML) has the surface Fermi level shifted toward the conduction band minimum for n-type InGaAs, but near the valence band maximum for p-type InGaAs. This is consistent with the HfO_2/InGaAs(0 0 1)−(4×2) interface being at least partially unpinned, i.e., a low density of states in the band gap. The partially unpinned interface results from the modest strength of the bonding between HfO_2 and InGaAs(0 0 1)−(4×2) that prevents substrate atom disruption. The fortuitous structure of HfO_2 on InAs(0 0 1)−(4×2) and InGaAs(0 0 1)−(4×2) allows for the elimination of the partially filled dangling bonds on the surface, which are usually responsible for Fermi level pinning. © *2010 American Institute of Physics*. [doi:10.1063/1.3427584]

I. INTRODUCTION

As complementary metal oxide semiconductor (CMOS) technology transitions from the traditional silicon based materials for the 45 nm node and beyond, both high-κ dielectrics and III-V semiconductors warrant investigation. Hafnium-based materials are already being incorporated[1,2] as the gate insulator for production of metal oxide semiconductor field effect transistors (MOSFETs) due to their much higher dielectric constants compared to SiO_2 and large band offsets with most semiconductors.[3–5] InGaAs has a lower band gap than silicon and shows higher electron mobility in experimental device architectures, making it an attractive material for increasing CMOS performance at low supply voltages.[6,7]

Unlike the Si/SiO_2 interface, which has the beneficial characteristics of a low density of interfacial states (D_{it}) when formed by thermal oxidation of Si followed by hydrogen passivation, the InGaAs/HfO_2 interface must be created through oxide deposition. Furthermore, the oxide deposition must leave the interface electrically passive with low D_{it} so that the Fermi level is unpinned (low state density in the band gap) allowing the applied gate voltage to provide a high on/off source-drain current ratio. Many methods have been investigated for HfO_2 deposition, which include molecular beam epitaxy (MBE) methods,[8,9] physical vapor deposition (PVD) methods,[10–12] e^- beam deposition,[13–17] and atomic layer deposition.[18–20] Some methods incorporate a protective interlayer between the III-V and the oxide, which has shown some success.[10,12,15] However, these methods frequently neglect to consider the III-V surface reconstruction and many do not maintain ultrahigh vacuum (UHV) conditions during interface formation. This study shows that by strictly controlling the InGaAs surface reconstruction prior to deposition and the UHV conditions, the Fermi level can be at least partially unpinned because control can be exerted over the type of bonding between the semiconductor and oxide.

$In_{0.53}Ga_{0.47}As$(0 0 1) is grown via MBE latticed-matched to InP(0 0 1). The group III rich surface of $In_{0.53}Ga_{0.47}As$(0 0 1)/InP(0 0 1) has (4×2) periodicity,[21,22] and this surface reconstruction is discussed in detail elsewhere.[23] Its main features are In/Ga row and trough structures oriented in the [1 1 0] direction with a row separation of ∼17 Å. This structure is remarkably similar to the InAs(0 0 1)−(4×2) surface, as shown by detailed STM studies on both surfaces, which is discussed in detail

---

[a)] Electronic mail: jclemens@ucsd.edu. Tel.: (858) 534-3498.
[b)] Electronic mail: sbishop@ucsd.edu. Tel.: (858) 534-9505.
[c)] Electronic mail: joonslee@ucsd.edu. Tel.: (858) 534-9506.
[d)] Author to whom correspondence should be addressed. Electronic mail: akummel@ucsd.edu. Tel.: (858) 534-3368.
[e)] Electronic mail: rdroopad@txstate.edu. Tel.: (512) 245-6165.

0021-9606/2010/132(24)/244701/8/$30.00

elsewhere.[24,25] The InAs(0 0 1)$-(4\times2)$ surface shows better long range order, has larger mean domain sizes, and has fewer defects. The InAs(0 0 1)$-(4\times2)$ surface is a better substrate than $In_{0.53}Ga_{0.47}As$(0 0 1)$-(4\times2)$ for the identification of specific bonding geometries of chemisorbates since InAs(0 0 1)$-(4\times2)$ offers better resolution in the trough region and lower defect density. A $c(8\times2)$ periodicity coexists on both surfaces that is chemically nearly identical to the (4×2) surfaces.[21,23,25] For simplicity, only the (4×2) notation is used herein for the group III rich surfaces of InAs(0 0 1) and $In_{0.53}Ga_{0.47}As$(0 0 1).

Both InGaAs(0 0 1)$-(4\times2)$ and InAs(0 0 1)$-(4\times2)$ are used to study the deposition of Hf and HfO_2 and the resulting interfaces. The chemical similarity of these two surfaces suggests many results are mutually analogous. The similarity of these two III-V surfaces is further reflected in their nearly identical symmetry changes at lower temperatures.[23,24] However, the band gap of $In_{0.53}Ga_{0.47}As$ is about 2× larger than that of InAs (0.73 eV instead of 0.35 eV); consequently, measuring the surface Fermi level position with respect to the valence and conduction band edges [valence band maximum (VBM) and conduction band minimum (CBM), respectively] using scanning tunneling spectroscopy (STS) is far more reliable on InGaAs than InAs. This higher reliability of the position of the Fermi level within the band gap (i.e., n-type versus p-type behavior) is especially critical for the STS technique since the accuracy is only about ±0.1 eV under most circumstances.

MOSFETs operate by an external electric field from the gate changing the position of the Fermi level in the semiconductor relative to the VBM and CBM. When there are states in the band gap, the external field cannot change the filling of states in the conduction or valance bands and instead the external field only induces minor changes in the filling of the defect states; this is denoted as "Fermi level pinning." These midgap states are usually created by dangling bonds—partially filled nonbonding orbitals on the semiconductor surfaces—or by highly ionic bonds.[26,27] In order for an oxide/semiconductor interface to be electrically "passive," the interface must have a very low density of defect states ($<10^{12}$ cm^{-2} eV^{-1}). To form a passive surface, the oxide deposition must not only avoid displacing surface atoms, since displaced atoms usually have partially filled dangling bonds, but the oxide/semiconductor bonding structure must eliminate any partially filled dangling bonds on the clean semiconductor surface without creating highly ionic bonds. By comparing two different methods of depositing a given oxide, HfO_2, the role of the deposition method in atomic displacement of substrate atoms in oxide/semiconductor bond formation is revealed. Both InGaAs(0 0 1)$-(4\times2)$ and InAs(0 0 1)$-(4\times2)$ have pinned electronic structures on their clean surfaces so an oxide needs to eliminate the dangling bonds responsible for the midgap states to passivate the surface. Furthermore, the bonds between the metal oxide and the surface cannot be strong highly ionic bonds since these tend to also create midgap states. By determining the atomic and electronic structure of an oxide that partially passivates these surfaces, it is possible to understand the types of bonds to metal (Hf) and oxygen that remove dangling bonds without creating new midgap states.

II. EXPERIMENTAL DETAILS

The experiments were performed in an UHV chamber equipped with an Omicron low-temperature scanning tunneling microscope, a PerkinElmer model 11-500 A Auger electron spectrometer, and an Omicron SpectraLEED low energy electron diffractometer. The base pressure was 2×10^{-11} Torr. The InAs samples were grown via MBE on commercially available InAs substrates as described elsewhere.[28] The $In_{0.53}Ga_{0.47}As$ samples were grown via MBE by collaborators offsite on commercially available InP substrates. The MBE grown layers were 1.5 μm thick, and the doping concentration was 1.5×10^{18} cm^{-3} for both p-type and n-type wafers, using Be or Si as dopants, respectively. The samples were protected with an amorphous As_2 capping layer (60–100 nm thick) and shipped in rough vacuum. After transfer into the UHV analysis chamber, the samples were degassed at 200 °C for 3 h and heated to 380 °C for 2 h to desorb the As_2 capping layer. The InAs(0 0 1)$-(4\times2)$ reconstruction was formed by increasing the substrate temperature by ~0.2 °C s^{-1} to 450 °C and holding for 10 min. The InGaAs samples were heating instead to a maximum temperature of 465 °C to obtain the (4×2) reconstruction. Surface periodicity was confirmed using low energy electron diffraction (LEED) and scanning tunneling microscopy (STM).

Hafnium was evaporated from a 99.9% purity metal rod using an Oxford Applied Research HPEB4 electron beam evaporator. Hafnium oxide was evaporated from a 99.9% purity oxide tablet using an MDC e-vap 3000 electron beam evaporator. Both evaporators were located in a differentially pumped chamber at a base pressure of $\sim5\times10^{-9}$ Torr. Reactive oxidation of the Hf/InAs(0 0 1)$-(4\times2)$ was achieved by introducing 99.994% purity O_2 into the UHV chamber through a UHV leak valve at pressures between 1×10^{-8} and 1×10^{-6} Torr.

Filled state STM images were acquired at -1.50 to -3.00 V sample bias relative to the electrochemically etched W tip. The constant-current images were taken at a tunneling current setpoint of 50–100 pA. STS was performed using a lock-in amplifier (with a sine wave reference signal of 50 mV and 1.5 kHz) to obtain the dI/dV data from the I(V) output of the Omicron MATRIX electronics. Several ($\sim5-10$) dI/dV curves are averaged together and reported in the STS data.

III. RESULTS AND DISCUSSION

A. Reactive Oxidation of Hf on InAs(0 0 1)$-(4\times2)$

Figure 1(a) shows STM results for room temperature deposition of Hf metal on InAs(0 0 1)$-(4\times2)$ at low coverage. Single chemisorption sites are identified for Hf atoms (green arrows), although larger clusters are also apparent. High resolution STM images reveal two nearly equivalent Hf addition sites that both occupy locations on the side of the rows, and are identified as the row-edge [Fig. 1(b)] and

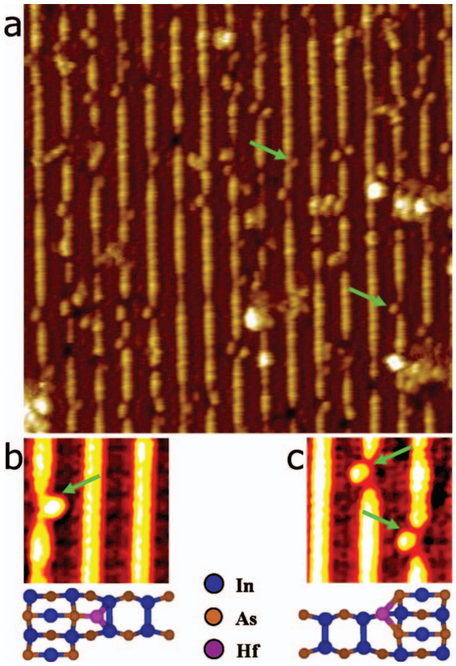

FIG. 1. (a) 270 Å×270 Å STM image (−1.5 V, 100 pA) of the low coverage Hf/InAs(0 0 1)−(4×2) surface showing the side-of-row Hf single atom addition sites, which are highlighted by the green arrows. (b) 50 Å×50 Å high resolution STM image (−2.0 V, 100 pA) of the row-edge Hf site and the corresponding proposed ball and stick diagram of this site on the $\beta3'(4\times2)$ reconstruction of the InAs(0 0 1) surface. (c) 50 Å×50 Å high resolution STM image (−2.0 V, 100 pA) of the As-bridge Hf site and the corresponding proposed ball and stick diagram of this site on the $\beta3'(4\times2)$ reconstruction of the InAs(0 0 1) surface. The contrast in [(b) and (c)] has been adjusted to optimize viewing of the structure in the trough.

As-bridge sites [Fig. 1(c)]. The row-edge site involves the Hf atom bonding adjacent to the row and protruding over the In–In dimer in the trough region, centered between the In atoms of the trough dimer. The As bridge site is distinguished from the row-edge site by the position of the Hf atom with respect to the In dimers in the trough. In the case of the As-bridge site, the Hf atom is between the In dimers rather than over one dimer and this position would cause it to bridge the neighboring row-edge As atoms. Proposed bonding geometries for the row-edge and As-bridge sites are shown in the ball and stick diagrams in the lower portions of Figs. 1(b) and 1(c). Nearly all other Hf sites on the surface are either simple combinations of these two sites or are high coverage sites with an unresolved structure. The single sites are studied for their oxidation properties since their structures are more readily identified.

Molecular oxygen was introduced into the STM chamber to observe oxidation of the single Hf addition sites on InAs(0 0 1)−(4×2) *in situ*. A single Hf atom chemisorption site was considered to be oxidized when its appearance changed in the STM image. The unoxidized Hf sites are readily distinguished from the oxidized single HfO_x sites (not shown); the unoxidized single Hf sites are circular in filled state STM images with a height of ~0.3 Å above the row structure while the HfO_x sites change in shape and apparent height above the row structure.

The single Hf atoms were shown to have very low reactivity to O_2 when chemisorbed to the InAs surface; only 20% ± 10% of the single Hf atoms were oxidized after a total O_2 dose of 700 L, as obtained from one *in situ* oxidation experiment that tracked 26 Hf addition sites. The large uncertainty is due to the difficulty in counting and tracking reaction sites in STM data throughout the 35 consecutive images. Furthermore, reaction of O_2 with the clean InAs substrate was observed, consistent with the previously observed mechanism.[28]

The low reactivity for O_2 on isolated Hf atoms (sticking probability of $1-4\times10^{-4}$) is probably due to Hf having a lower electronegativity than the In and As atoms of the substrate; therefore, it is likely that Hf has donated electron density when bonding to the surface. On other semiconductor surfaces, O_2 dissociatively chemisorbs via charge addition to its π^* antibonding orbital.[29–31] The low reaction probability of O_2 on Hf atoms is consistent with isolated Hf atoms providing little weakly bound electron density available for transfer to the incoming O_2 molecule to accept into its π^* orbital. The sticking probability for O_2 on clean InAs(0 0 1)−(4×2) is $\sim10^{-4}$.[28] The O_2 reaction on clean InAs(0 0 1)−(4×2) involves the displacement of As atoms to form In–O–In bonds; it is likely that these displacement reactions will pin the Fermi level so it is imperative to find a method of increasing the Hf reactivity relative to the substrate.

After annealing the unoxidized low coverage Hf/InAs(0 0 1)−(4×2) surface to 400 °C, the single Hf atoms coalesce into islands [Fig. 2(a)]. The smallest islands consist of six Hf atoms, or Hf hexamers and one is shown in the inset of Fig. 2(a). Larger Hf islands exist on the surface, however, no smaller Hf islands appear after annealing, which indicates that the hexamers are the smallest stable islands for the conditions. A proposed ball and stick model for the Hf hexamer on InAs(0 0 1)−(4×2) is shown in Fig. 2(d). The standard allotrope of Hf forms a hexagonal close packed (hcp) crystal structure;[32] as the Hf islands increase in size beyond six atoms, they begin to lack atomic corrugation in STM and appear as bright featureless regions. The difficulty in resolving atomic corrugation of the islands in STM is consistent with the Hf bonding closely together, as in the hcp structure.

The hexamers and larger Hf islands are more reactive toward O_2 than the single Hf atoms, consistent with their having a metallic character. After an equivalent 700 L dose of O_2, 64% ± 7% of the 14 hexamer islands observed reacted with O_2, and 60% of the reaction occurred within the first 100 L of O_2 exposure. Similar criteria employed for oxidation of the single Hf addition sites were used to determine whether a Hf hexamer was oxidized. The unoxidized Hf hexamer islands have a length of ~24 Å and a height of ~0.5 Å above the row structure, while the oxidized islands have an irregular shape and appear much higher in STM images. Figure 2(b) shows a group of Hf hexamers (green arrows) on the InAs(0 0 1)−(4×2) surface before O_2 is introduced into the UHV chamber. Figure 2(c) is the *same area of the surface* after 350 L O_2 exposure, showing the resulting oxidation. The oxidized hexamers in Fig. 2(c) showed an increase in apparent STM height of about 1.5 Å

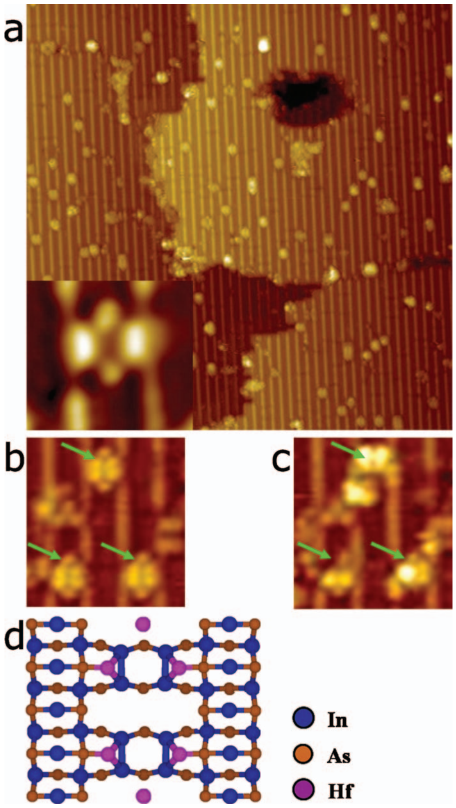

FIG. 2. (a) 770 Å × 770 Å STM image (−2.0 V, 100 pA) of the of the low coverage Hf/InAs$(0\ 0\ 1)-(4\times2)$ surface after being annealed to 400 °C, showing that the Hf coalesces into islands of ≥6 atoms. Inset: detail of one Hf hexamer. (b) High resolution 70 Å × 70 Å STM image (−2.0 V, 100 pA) of a group of three Hf hexamers before exposure to O_2, indicated by green arrows. (c) High resolution 70 × 70 $Å^2$ STM image (−2.0 V, 100 pA) of the *same region of the surface* after exposure to 350 L O_2. The oxidation of the Hf hexamers is evident, indicated by green arrows. d) The ball and stick diagram of the proposed Hf hexamer geometry.

from Fig. 2(b). The uniform oxidation of the Hf hexamers contrasts with the oxidation of the single Hf atoms, which showed only sporadic single oxidation events throughout the O_2 exposure time.

The annealed Hf-deposited surface shows high selectivity for oxidation of the Hf over the III-V substrate. After oxidation of the Hf islands, the surface was annealed at 400 °C to attempt to form a more ordered overlayer of HfO_x on the InAs surface. Some local order is observed, but the majority of the regrowth shows amorphous island formation (Fig. 3). Although the exact structure cannot be determined since the island is amorphous, it is identified as an oxide based on the height increase during oxidation as explained above. The amorphous island formation is consistent with a preferential bonding of the HfO_x to itself, rather than the InAs(0 0 1) substrate. The mobility of the HfO_x on the surface at 400 °C is also consistent with relatively weak bonding between the HfO_x and the substrate.

B. Direct deposition of HfO_2 on InAs$(0\ 0\ 1)-(4\times2)$ and InGaAs$(0\ 0\ 1)-(4\times2)$

On InAs$(0\ 0\ 1)-(4\times2)$ at 200 °C, low coverage of HfO_2 deposited via e^- beam evaporation is shown in the STM data in Fig. 4(a). This image contains only the lowest-coverage sites, whose bonging structure is more readily identified than for larger sites. The HfO_2 bonds to itself in a variety of structures, making identification of specific molecular structures for the larger sites more challenging. The smallest sites (∼8 Å in diameter) are attributed to HfO_2 molecules bonding on the side of the rows and over the trough regions, observed either singly or in pairs of bridging sites.

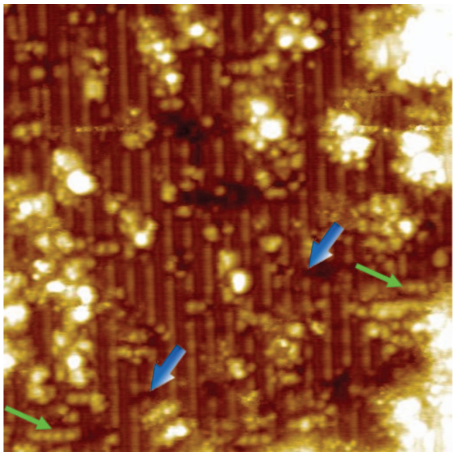

FIG. 3. 390 × 390 $Å^2$ STM image of the Hf/InAs$(0\ 0\ 1)-(4\times2)$ surface after oxidation by 480 L O_2 at 25 °C and subsequent anneal at 400 °C for 10 min (−2.10 V, 50 pA). The green arrows show regions of first layer growth ordered in the $[-1\ 1\ 0]$ direction and the blue arrows show oxygen sites (dark cuts in the rows), consistent with Ref. 28.

In the low coverage regime, HfO_2 is often observed in STM as double, row "bridge" sites as shown in the blue box of Fig. 4(a). These specific chemisorption sites have been modeled using density functional theory (DFT), and those results are published in a companion paper.[33] In that paper, DFT results reveal that the double HfO_2 bridge site is slightly more stable than the single HfO_2 half-bridge "row edge" site by about 0.4 eV/HfO_2 molecule. This is consistent with the STM results, showing the population of bridge sites is larger than one would expect by a random distribution of single sites. In STM images, single HfO_2 sites appear different than the single Hf atom sites—the HfO_2 sites are slightly larger in diameter and higher above the row. The DFT calculations of *Bishop et al.*[33] show that the lowest energy bonding structure for a HfO_2 molecule is for it to be oriented over the trough region, along the side of the row via O–In bonds and Hf–As bonds. This bonding configuration is illustrated in the ball and stick diagram of the half-bridge row-edge site in Fig. 4(b). On the clean surface, the substrate atoms for these sites all have dangling bonds that result from their tricoordinated configuration. The proposed HfO_2 site shown in Fig. 4(b) would eliminate these dangling bonds on the row-edge As atoms and trough-dimer In atoms.

At higher coverages, a Volmer–Weber growth mode is observed with small HfO_2 islands forming on the InAs$(0\ 0\ 1)-(4\times2)$ surface for substrate temperatures of 200 °C during e^- beam HfO_2 deposition. This is represented in the STM data in Fig. 4(c) and the corresponding histogram of the pixel heights. For the coverage in Fig. 4(c), 14% of the surface area is first layer growth and 11% is second layer growth or higher, typical for Volmer–Weber growth.[34] The

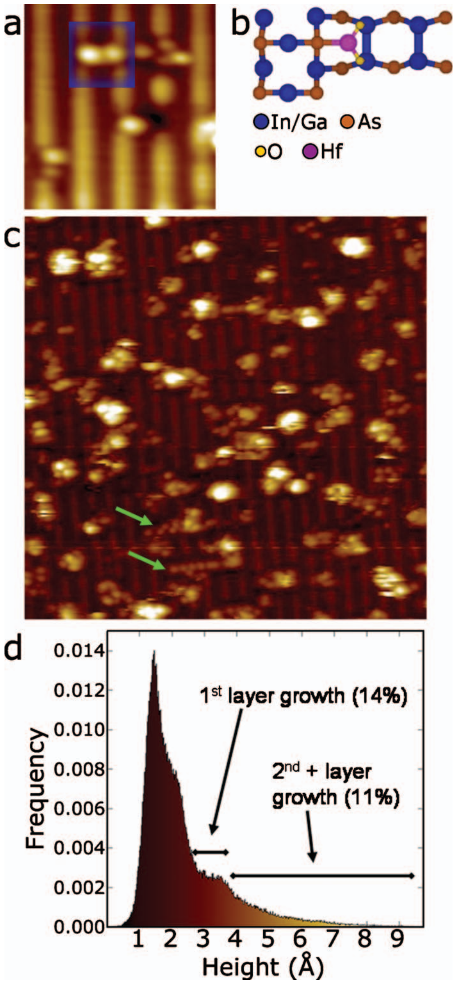

FIG. 4. Electron beam deposition of HfO_2 on $InAs(0\ 0\ 1)-(4\times2)$. (a) 90×80 Å^2 STM image of the HfO_2 bridge site (blue box) and other single HfO_2 sites (−2.5 V, 30 pA). The deposition temperature was 200 °C. (b) The ball and stick diagram of a single HfO_2 half-bridge (row-edge) site. (c) 390×390 Å^2 STM image of submonolayer growth of HfO_2 by e^- beam deposition at a substrate temperature of 200 °C (−3.5 V, 50 pA). The green arrows show the ordered first layer growth. (d) A histogram of the pixel heights for the image in Fig. 4(c). Fourteen percent of the surface area is first layer HfO_2 growth and 11% of the surface area is multilayer growth. These ratios are consistent with a Volmer–Weber growth mode.

first layer growth shows small regions of order, indicated by the green arrows in Fig. 4(c). This ordered reconstruction was observed to be more prevalent at higher deposition or annealing temperatures (≥300 °C). Deposition of HfO_2 via e^- beam is known to produce polycrystalline films for elevated temperatures of >250 °C and smooth, amorphous films at lower temperatures.[17,35] This study is consistent with those results.

At higher coverage of HfO_2 on the group III rich $InAs(0\ 0\ 1)$ or $InGaAs(0\ 0\ 1)$ surfaces, the growth is amorphous at substrate temperatures up to ~200 °C. Since the growth mode is Volmer–Weber-like, full coverage only occurs after the equivalent of several monolayers of oxide has been deposited. For an annealing temperature of 100 °C, full coverage of HfO_2 on the $InGaAs(0\ 0\ 1)-(4\times2)$ surface [Fig. 5(a)] shows smooth, amorphous growth with an rms roughness of 0.8 Å. Similar results are seen for the $InAs(0\ 0\ 1)-(4\times2)$ surface (not shown).

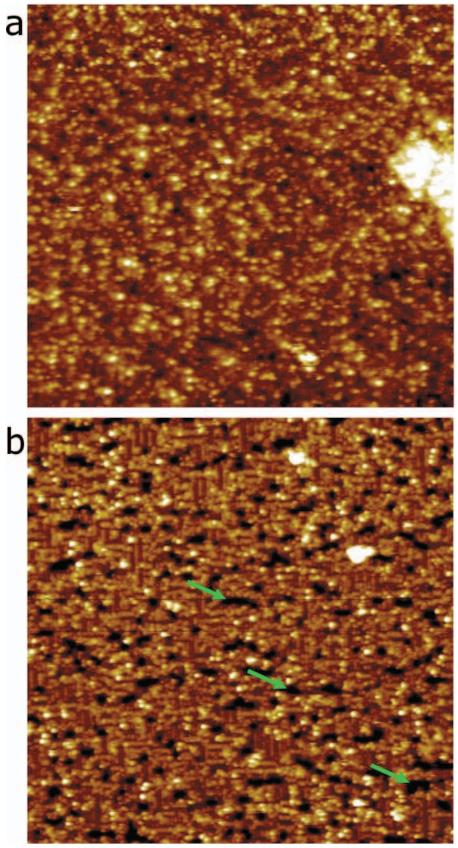

FIG. 5. (a) 820×870 Å^2 STM image (−2.5 V, 50 pA) of the full coverage $HfO_2/InGaAs(0\ 0\ 1)-(4\times2)$ surface showing the smooth amorphous growth with rms roughness of 0.8 Å. The substrate temperature was 25 °C followed by a 100 °C anneal and the growth rate is approximately 0.2 ML s^{-1}. (b) 870×870 Å^2 STM image (−2.3 V, 50 pA) of a ~0.8 ML $HfO_2/InGaAs(0\ 0\ 1)-(4\times2)$ surface after annealing to 300 °C. There is more ordered structure in the first layer growth, but also potential substrate atom displacement (green arrows).

At annealing or deposition temperatures of 300 °C, the HfO_2 on $InGaAs(0\ 0\ 1)-(4\times2)$ shows small regions of ordered structures that are only in the first layer and also disordered, multilayer island growth [Fig. 5(b)]. These first layer ordered regions are similar to the ordered regions formed by oxidation of the annealed Hf atoms on the $InAs(0\ 0\ 1)-(4\times2)$ surface (Fig. 3, green arrows). However e^- beam deposited HfO_2 may also induce substrate roughening, as evidenced by the dark pits in the STM image of the $HfO_2/InGaAs(0\ 0\ 1)-(4\times2)$ surface [Fig. 5(b), green arrows].

While amorphous gate oxides are usually preferable for MOSFETs, an ordered first layer of gate oxide is usually desired.[36] An ordered first layer is often optimal since it will allow further oxide growth to have uniform thickness without pinholes and because ordered structures are more likely to leave the surface unpinned. The first-layer order seen in Fig. 5(b) suggests that the HfO_2 bonds to the III-V substrate are relatively weak; the diffusion of HfO_2 on the surface to form these ordered regions would not be likely to occur for this refractory oxide if the bonds to the substrate were strong. DFT calculations by Bishop *et al.*[33] show that the chemisorption energy of the HfO_2 molecule to the III-V surface is

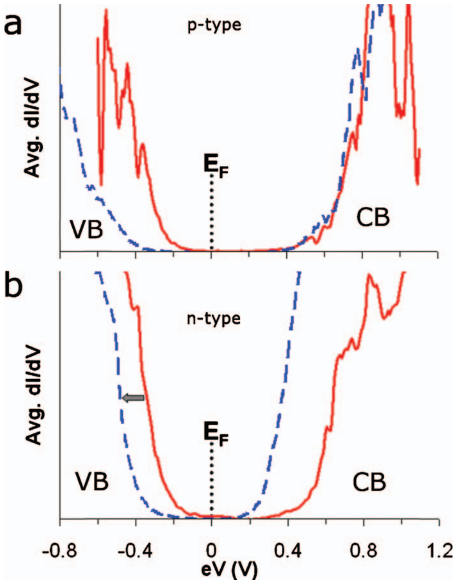

FIG. 6. (a) The STS results for clean (red solid line) vs full coverage of HfO_2 (blue dashed line) on p-type InGaAs(0 0 1)$-(4\times2)$ using e^- beam deposition at 25 °C and subsequent 100 °C anneal. The E_F position remains at 0.5 eV below the CBM, consistent with an unpinned interface.(b) The STS results for clean (red solid line) vs full coverage of HfO_2 (blue dashed line) on n-type InGaAs(0 0 1)$-(4\times2)$. The E_F position shifts with respect to both the VBM and CBM, which is consistent with the HfO_2 interface partially removing the p-type pinning behavior associated with the clean InGaAs surface.

3.95–4.34 eV, which corresponds to only ~1.4 eV per bond since the HfO_2 makes three bonds to the surface.

STS was performed on full-coverage HfO_2/InGaAs(0 0 1)$-(4\times2)$ for both p-type and n-type substrates and compared to STS results for the clean InGaAs(0 0 1)$-(4\times2)$ surfaces. As previously stated, the STS experiments were only performed on InGaAs(0 0 1) since the small band gap of InAs(001) inhibits precise determination of the Fermi level energy shift with respect to the band edges on InAs(001), especially for surfaces with the rough topology induced by oxide deposition.

For the clean surface, both n-type and p-type InGaAs(0 0 1)$-(4\times2)$ show dI/dV curves that indicate that the surface Fermi level (E_F) is located near the VBM, as shown in Figs. 6(a) and 6(b) (red lines). In each case, E_F =VBM+0.2 eV. This apparent p-type character for n-type InGaAs(0 0 1)$-(4\times2)$ is likely due to pinning induced by defect states on the clean surface.[23] The p-type character of both InGaAs surfaces is reproducible in STS experiments and is described as being "pinned p-type."

After full-coverage deposition of HfO_2 (substrate temperature of 25 °C followed by a 100 °C anneal and a growth rate of ~0.2 ML s^{-1}), the STS results show at least a partial unpinning of the surface. The blue dashed line in Fig. 6(a) (p-type InGaAs) is the STS data after oxide deposition; the results show that the CBM position remains nearly the same with respect to E_F, but the valence band-edge density decreases. The origin of this decrease in valence band-edge density on the p-type material is unknown and does not occur with the n-type material, but the difference could be due to irregularities in the thickness of the oxide layer. In Fig. 6(b) (n-type InGaAs), the Fermi level position shifts with respect to both the CBM and VBM, consistent with a partially unpinned surface Fermi level (blue dashed line). The overall shift is only about 0.2 eV. It appears that the band gap was *reduced* in this case by 0.1 eV. However, the band gap is still close to the expected value (0.73 eV) and the Fermi level position clearly moves toward the CBM and away from the VBM.

Consistent with a partially unpinned interface, the STS results for HfO_2 on p-type InGaAs(0 0 1)$-(4\times2)$ show no change for the Fermi level position with respect to the CBM (E_F=CBM−0.5 eV), while the STS results for HfO_2 on n-type InGaAs(0 0 1)$-(4\times2)$ show that the Fermi level moves from 0.5 eV below the CBM to 0.2 eV below the CBM. Additionally, for HfO_2 on n-type InGaAs(0 0 1) $-(4\times2)$, the Fermi level position moves from VBM +0.2 eV to VBM+0.4 eV. These results suggest that a partially unpinned interface is formed between HfO_2 and InGaAs(0 0 1)$-(4\times2)$ for the conditions of low annealing temperature (≤200 °C). At higher annealing temperatures (≥300 °C), the Fermi level position on n-type material is not as close to the CBM and appears more p-type. This is likely related to the substrate roughening seen for 300 °C annealed HfO_2/InGaAs(0 0 1)$-(4\times2)$. For p-type material and higher annealing temperatures, the Fermi level position remains near the VBM. For low annealing and deposition temperature (<200 °C), the unpinning may not be complete due to oxidation of the III-V substrate during deposition. The background pressure during e^- beam deposition reaches the range of 10^{-6} Torr in the differentially pumped evaporation chamber, indicating that the HfO_2 evaporates incongruently. Adventitious oxygen species could chemisorb onto the InGaAs surface and create pinning states. Oxygen-induced pinning has been seen for other III-V surfaces.[27] Investigation is warranted of other deposition methods (atomic layer deposition) since the reactions may involve less adventitious O_2 and the undesired arsenic oxide "clean up" effect has been observed for other high-κ oxide metal precursors such as trimethylaluminum.[37,38]

The partial unpinning of InGaAs(0 0 1)$-(4\times2)$ is very instructive for identifying other possible oxide-semiconductor unpinned interfaces. The only other STM study that showed the atomic positions for an unpinned interface was Ga_2O/GaAs(0 0 1)$-(2\times4)$ where the Ga_2O made simple Ga–As bonds to the surface; the surface was unpinned by just forming a bulklike transition to the oxide.[27,39] For HfO_2/InGaAs(1 0 0)$-(4\times2)$, the interfacial bonds are not bulklike; instead they are Hf–As bonds and O–In/Ga bonds.[33] Strong highly ionic bonds are expected to create midgap states which pin the interface, but this does not occur for HfO_2/InGaAs(0 0 1)$-(4\times2)$. Instead the bonds are relatively weak, as shown by the formation of some locally ordered regions at medium coverage. This relatively weak bonding to the surface occurs because the HfO_2 formula units already have cationic-anionic charge exchange. Furthermore, the fortuitous structure of HfO_2 allows elimination of the partially filled dangling bonds on the surface which are thought to be responsible for Fermi level pinning of InGaAs(0 0 1)$-(4\times2)$ even on the defect free surface.

IV. CONCLUSION

In this study, deposition methods for HfO_2 on two different III-V substrates were examined and their combined results reveal complementary aspects of the oxide/semiconductor interface formation. This approach takes advantage of the low defect density of $InAs(0\ 0\ 1)-(4\times2)$ for atomic structure identification and the larger band gap of $In_{0.53}Ga_{0.47}As(0\ 0\ 1)-(4\times2)$ for electronic structure determination.

Oxidation of Hf metal on the $InAs(0\ 0\ 1)-(4\times2)$ surface was observed *in situ* via STM. Two different single atom Hf chemisorption sites were identified on the $InAs(0\ 0\ 1)-(4\times2)$ surface, but these single atom addition sites had low reactivity to O_2. Annealing the $Hf/InAs(0\ 0\ 1)-(4\times2)$ surface created Hf clusters, the smallest of which was six atoms in size. These hexamers and other larger Hf islands were reactive to O_2, but selectivity over the substrate for oxidation may be problematic. The direct e^- beam deposition of HfO_2 is preferable for interface formation.

Single chemisorption sites for e^- beam deposited HfO_2 on $In(Ga)As(0\ 0\ 1)-(4\times2)$ were identified that occur on the side of the rows and over the trough regions. Thicker layer growth of HfO_2 occurs via a Volmer–Weber-like process where there is a preference for the HfO_2 to form islands on the III-V surface. The STS (electronic structure) results show that full coverage of HfO_2 annealed below 200 °C on $In_{0.53}Ga_{0.47}As(0\ 0\ 1)-(4\times2)$ moves the E_F further from the VBM and closer to the CBM for n-type InGaAs. The Fermi level is unchanged with respect to the CBM for p-type InGaAs. The STS results suggest that the p-type pinning observed on clean $InGaAs(0\ 0\ 1)-(4\times2)$ is partially removed upon the formation of an interface with HfO_2. If the surface could be protected from adventitious O_2 chemisorption during deposition, full unpinning would likely be possible for deposition below 200 °C. The partial unpinning of the interface results from the modest strength of the bonding between HfO_2 and $InGaAs(0\ 0\ 1)-(4\times2)$, preventing surface disruption at these low annealing temperatures. Theoretical results in the companion paper further support that the fortuitous structure of HfO_2 allows for the elimination of the partially filled dangling bonds on the surface by formation of both Hf-As bonds and O-In/Ga bonds.[33]

ACKNOWLEDGMENTS

This work was financially supported by The Semiconductor Research Corporation (Grant No. SRC-NCRC-1437.003), The Materials Structures and Devices Focus Center (Grant No. FCRP-MSD-887.011), and The National Science Foundation (Grant No. NSF-DMR 0706243).

[1] J. Markoff, The New York Times (online version), Jan. 27, 2007.
[2] M. LaPedus, EE Times (online version), Feb. 5, 2007.
[3] P. W. Peacock and J. Robertson, Phys. Rev. Lett. **92**, 057601 (2004).
[4] S. Sayan, E. Garfunkel, and S. Suzer, Appl. Phys. Lett. **80**, 2135 (2002).
[5] J. Robertson and B. Falabretti, J. Appl. Phys. **100**, 014111 (2006).
[6] Y. Xuan, Y. Q. Wu, and P. D. Ye, IEEE Electron Device Lett. **29**, 294 (2008).
[7] S. Koveshnikov, N. Goel, P. Majhi, C. K. Gaspe, M. B. Santos, S. Oktyabrsky, V. Tokranov, M. Yakimov, R. Kambhampati, H. Bakhru, F. Zhu, J. Lee, and W. Tsai, 2008 66th Annual Device Research Conference, 2008, p. 43.
[8] Y. N. Sun, E. W. Kiewra, S. J. Koester, N. Ruiz, A. Callegari, K. E. Fogel, D. K. Sadana, J. Fompeyrine, D. J. Webb, J. P. Locquet, M. Sousa, R. Germann, K. T. Shiu, and S. R. Forrest, IEEE Electron Device Lett. **28**, 473 (2007).
[9] Z. J. Yan, R. Xu, Y. Y. Wang, S. Chen, Y. L. Fan, and Z. M. Jiang, Appl. Phys. Lett. **85**, 85 (2004).
[10] I. Ok, H. Kim, M. Zhang, F. Zhu, S. Park, J. Yum, H. Zhao, D. Garcia, P. Majhi, N. Goel, W. Tsai, C. K. Gaspe, M. B. Santos, and J. C. Lee, Appl. Phys. Lett. **92**, 202903 (2008).
[11] I. Ok, H. Kim, M. Zhang, F. Zhu, S. Park, J. Yum, H. Zhao, D. Garcia, P. Majhi, N. Goel, W. Tsai, C. K. Gaspe, M. B. Santos, and J. C. Lee, Appl. Phys. Lett. **92**, 112904 (2008).
[12] S. Koveshnikov, W. Tsai, I. Ok, J. C. Lee, V. Torkanov, M. Yakimov, and S. Oktyabrsky, Appl. Phys. Lett. **88**, 022106 (2006).
[13] C. H. Hsu, P. Chang, W. C. Lee, Z. K. Yang, Y. J. Lee, M. Hong, J. Kwo, C. M. Huang, and H. Y. Lee, Appl. Phys. Lett. **89**, 122907 (2006).
[14] K. Cherkaoui, S. Monaghan, M. A. Negara, M. Modreanu, P. K. Hurley, D. O'Connell, S. McDonnell, G. Hughes, S. Wright, R. C. Barklie, P. Bailey, and T. C. Q. Noakes, J. Appl. Phys. **104**, 064113 (2008).
[15] C. H. Pan, J. Kwo, K. Y. Lee, W. C. Lee, L. K. Chu, M. L. Huang, Y. J. Lee, and M. Hong, J. Vac. Sci. Technol. B **26**, 1178 (2008).
[16] H. Harris, K. Choi, N. Mehta, A. Chandolu, N. Biswas, G. Kipshidze, S. Nikishin, S. Gangopadhyay, and H. Temkin, Appl. Phys. Lett. **81**, 1065 (2002).
[17] J. Ni, Z. C. Li, and Z. J. Zhang, Frontiers of Materials Science in China **2**, 381 (2008).
[18] R. D. Long, E. O'Connor, S. B. Newcomb, S. Monaghan, K. Cherkaoui, P. Casey, G. Hughes, K. K. Thomas, F. Chavlet, I. M. Povey, M. E. Pemble, and P. K. Hurley, J. Appl. Phys. **106**, 084508 (2009).
[19] D. Shahrjerdi, D. I. Garcia-Gutierrez, T. Akyol, S. R. Bank, E. Tutuc, J. C. Lee, and S. K. Banerjee, Appl. Phys. Lett. **91**, 193503 (2007).
[20] M. Kobayashi, P. T. Chen, Y. Sun, N. Goel, P. Majhi, M. Garner, W. Tsai, P. Pianetta, and Y. Nishi, Appl. Phys. Lett. **93**, 182103 (2008).
[21] U. Seidel, H. J. Schimper, Z. Kollonitsch, K. Moller, K. Schwarzburg, and T. Hannappel, J. Cryst. Growth **298**, 777 (2007).
[22] U. Seidel, B. E. Sagol, C. Pettenkofer, and T. Hannappel, Appl. Surf. Sci. **255**, 722 (2008).
[23] J. Shen, J. B. Clemens, D. L. Feldwinn, W. Melitz, T. Song, E. A. Chagarov, A. C. Kummel, and R. Droopad, "Structural and electronic properties of group III rich $In_{0.53}Ga_{0.47}As(0\ 0\ 1)$," Surf. Sci. (to be published).
[24] D. L. Feldwinn, J. B. Clemens, J. Shen, S. R. Bishop, T. J. Grassman, A. C. Kummel, R. Droopad, and M. Passlack, Surf. Sci. **603**, 3321 (2009).
[25] C. Kendrick, G. LeLay, and A. Kahn, Phys. Rev. B **54**, 17877 (1996).
[26] M. Houssa, E. Chagarov, and A. Kummel, MRS Bull. **34**, 504 (2009).
[27] D. L. Winn, M. J. Hale, T. J. Grassman, J. Z. Sexton, and A. C. Kummel, J. Chem. Phys. **127**, 134705 (2007).
[28] J. B. Clemens, S. R. Bishop, D. L. Feldwinn, R. Droopad, and A. C. Kummel, Surf. Sci. **603**, 2230 (2009).
[29] T. Miyake, S. Soeki, H. Kato, T. Nakamura, A. Namiki, H. Kamba, and T. Suzaki, Surf. Sci. **242**, 386 (1991).
[30] Y. Miyamoto and A. Oshiyama, Phys. Rev. B **43**, 9287 (1991).
[31] J. H. Rechtien, U. Imke, K. J. Snowdon, P. H. F. Reijnen, P. J. Vandenhoek, A. W. Kleyn, and A. Namiki, Nucl. Instrum. Methods Phys. Res. B **48**, 339 (1990).
[32] H. W. King, *CRC Handbook of Chemistry and Physics*, 89th ed. edited by D. R. Lide, (CRC, Boca Raton, FL/Taylor & Francis, London, 2009).
[33] S. R. Bishop, J. B. Clemens, E. A. Chagarov, and A. C. Kummel, "Theoretical analysis of initial adsorption of high-κ metal oxides on $In_{(x)}Ga_{(1-x)}As(0\ 0\ 1)-(4\times2)$ surfaces," J. Chem. Phys. (2010).
[34] W. K. Liu and M. B. Santos, *Thin Films: Heteroepitaxial Systems*, edited by J. A. Vanables (World Scientific, Singapore, 1999), Chap. 1.
[35] M. F. Al-Kuhaili, S. M. A. Durrani, and E. E. Khawaja, J. Phys. D **37**, 1254 (2004).
[36] R. Droopad, M. Passlack, N. England, K. Rajagopalan, J. Abrokwah, and A. Kummel, Microelectron. Eng. **80**, 138 (2005).

[37] M. M. Frank, G. D. Wilk, D. Starodub, T. Gustafsson, E. Garfunkel, Y. J. Chabal, J. Grazul, and D. A. Muller, Appl. Phys. Lett. **86**, 152904 (2005).

[38] C. L. Hinkle, A. M. Sonnet, E. M. Vogel, S. McDonnell, G. J. Hughes, M. Milojevic, B. Lee, F. S. Aguirre-Tostado, K. J. Choi, H. C. Kim, J. Kim, and R. M. Wallace, Appl. Phys. Lett. **92**, 071901 (2008).

[39] M. J. Hale, S. I. Yi, J. Z. Sexton, A. C. Kummel, and M. Passlack, J. Chem. Phys. **119**, 6719 (2003).